

GT2011-453+-

FLUE GAS RECIRCULATION OF THE ALSTOM SEQUENTIAL GAS TURBINE COMBUSTOR TESTED AT HIGH PRESSURE

Felix Guethe, Dragan Stankovic, Franklin Genin, Khawar Syed,
 Alstom Power, Baden, Switzerland
 Dieter Winkler
 University of Applied Sciences Northwestern Switzerland

Abstract

Concerning the efforts in reducing the impact of fossil fuel combustion on climate change for power production utilizing gas turbine engines Flue Gas Recirculation (FGR) in combination with post combustion carbon capture and storage (CCS) is one promising approach. In this technique part of the flue gas is recirculated and introduced back into the compressor inlet reducing the flue gas flow (to the CCS) and increasing CO₂ concentrations. Therefore FGR has a direct impact on the efficiency and size of the CO₂ capture plant, with significant impact on the total cost. However, operating a GT under depleted O₂ and increased CO₂ conditions extends the range of normal combustor experience into a new regime. High pressure combustion tests were performed on a full scale single burner reheat combustor high-pressure test rig. The impact of FGR on NO_x and CO emissions is analyzed and discussed in this paper. While NO_x emissions are reduced by FGR, CO emissions increase due to decreasing O₂ content although the SEV reheat combustor could be operated without problem over a wide range of operating conditions and FGR. A mechanism uncommon for GTs is identified whereby CO emissions increase at very high FGR ratios as stoichiometric conditions are approached. The feasibility to operate Alstom's reheat engine (GT24/GT26) under FGR conditions up to high FGR ratios is demonstrated. FGR can be seen as continuation of the sequential combustion system which already uses a combustor operating in vitiated air conditions. Particularly promising is the increased flexibility of the sequential combustion system allowing to address the limiting factors for FGR operation (stability and CO emissions) through separated combustion chambers.

Nomenclature

FGR	Flue gas recirculation
FGR-ratio	$\frac{\dot{m}_{recirculation}}{\dot{m}_{exhaust}}$
EV	(first) EnVironmental Burner
SEV	Sequential EnVironmental Burner
CCS	Carbon Capture and Storage
HRSG	Heat Recovery Steam Generator
HP, LP	High Pressure, Low Pressure
AFR	Air to fuel ratio (in kg/kg)
ϕ	fuel – air equivalence ratio
T _{flame}	adiabatic flame temperature
T _{hot gas}	hot gas temperature
T_SEV_IN	SEV combustor inlet temperature
P _{K2}	Pressure at EV inlet
T _{K2}	Temperature at EV inlet
τ_{ign}	auto-ignition time
t _{res}	combustor residence time
PDF	probability density function (PDF)
C2+	$\sum_n [C_n H_{2n+2}] \sim$ sum of higher alkane volumes fraction in natural gas mixture

Introduction

The change of global climate accompanied by the increase of global average temperatures as well as its anthropogenic nature are well documented [1]. Consequently changes in fuel consumption and pollutant emissions on large scale are required to prevent significant negative impact on our planets living conditions and human welfare. The most prominent effect on global warming is related to emitted CO₂, which is produced in combustion processes. While switching to renewable and carbon free energy production can be seen as a long

term goal, the use of carbon containing fuels as an important part of the global energy mix seems to be unavoidable at least in mid-term.

Consequently carbon capture and storage (CCS) technologies are to be developed to reduce the carbon foot print of conventional combustion based power generation. Principally CO₂ can be captured before or after the combustion process [2]. In the former case H₂ rich gases have to be burned, which is challenging due to its high reactivity. In the post combustion case the CO₂ is to be extracted from the flue gases requiring relatively large facilities. Recirculating the flue gases and further utilizing the remaining O₂ is therefore economically rewarding due to the reduced mass flows in the capture unit decreasing its size.

For gas turbines normally operating on natural gas the relative carbon content is already lower than for other fossil fuels. To contribute their share to the global CO₂ emission reduction GTs (with standard fuels) combined with combustion capture technologies including flue gas recirculation (FGR) have to be developed and implemented. This work investigates to what extent the usage of FGR is limiting the operational flexibility with respect to non FGR operation.

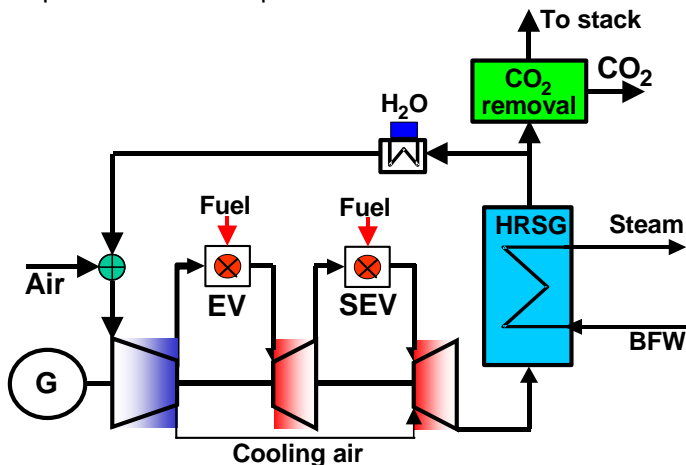


Figure 1: Schematic of a generic flue gas recirculation system on the example of Alstom's GT24/GT26 reheat engine.

The impact of FGR on a GT power plant and especially its combustion behavior had been described before by several authors [3, 4] including several manufacturers [5, 6, 7, 8] In general the effect on most components including the power outputs and efficiency is not very large. The effect on combustion is however significant with an advantage for lower NO_x emissions and more challenging conditions for blow out stability and CO emissions [8, 9].

An example of a reheat system is the Alstom reheat engine as is sketched for an FGR application in Figure 1 (from [8]): After the heat recovery steam generator (HRSG) part of the flue gas is recirculated and fed back into the GT inlet after passing through a cooler. The gas

at the GT-inlet is a mixture of air and flue gas with reduced O₂ and increased CO₂-content, which is after the compression mixed and burned with fuel in the combustor resulting also in altered exhaust gas composition with respect to the non-FGR engine. The reheat concept is described in [10] and uses two combustors in sequence: the EV ~ EnVironmental and the SEV ~ Sequential EV. The SEVs combustion behaviour is in many ways unconventional sine it is determined by autoignition and does not require stabilisation features.

The FGR ratio is defined as the ratio of mass of the recirculated gas to the GT exhaust mass flow, where the recirculated gas is determined either after the HRSG or after the cooler depending on the reference. The definition used here refers to mass flow after the HRSG [11].

In this paper the impact of FGR on the combustion process within a single SEV burner test rig is experimentally investigated at engine conditions. Implications for power output and operations will be addressed elsewhere [11].

For the CCS application, high FGR ratios are desirable to achieve the maximum CO₂ exit content and minimum exit mass flow. However the combustion process sets a limit due to the corresponding reduction in O₂ concentration. The latter yields challenges associated with combustion stability and the emission of incomplete combustion products. However a beneficial impact on NO_x emissions and fuel flexibility results. This will be highlighted later.

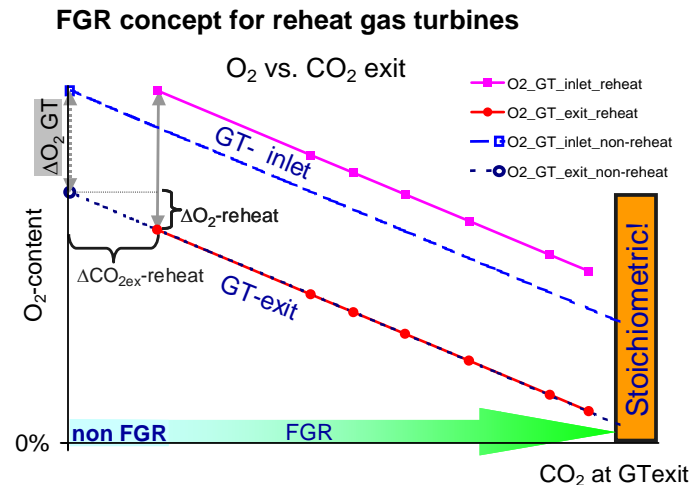


Figure 2: O₂ levels at GT inlet and exit vs. CO₂ at GT exit for sequential combustion system reheat engine and a non reheat engine.

For CCS applications the goal of FGR utilization is the increase of CO₂ content at decreased volume flow in the gas to be treated. The O₂ content at inlet and exit of the GT for varied FGR ratios are schematically given in Figure 2 plotted against the CO₂ content at the GT exit. It

should be highlighted that for comparison of different technologies within the framework of a FGR / CCS application the value of the FGR ratio is not as useful as the CO₂ exit concentration, which determines the CCS system. Dashed lines (and open symbols) depict O₂ concentrations for non-reheat engines at GT inlet and dotted lines at GT exit. The solid lines (full symbols) refer to O₂ concentrations of the reheat engine squares are used for inlet and circles for exit compositions. With increasing FGR CO₂ levels rise and O₂ is depleted. The O₂ exit vs. CO₂ exit content line characteristic (indicated by circles) is independent of the GT type (or AFR). The O₂ exit concentration is rather a function of stoichiometry for a given fuel and therefore falls on the same line for reheat and single combustor GT.

At the GT inlet the O₂-concentration (square symbols) decreases from the fresh air concentration with increasing FGR (moving along the dotted arrow from left to right) up to the theoretical limits determined by the stoichiometry of the combustor when no O₂ is left at the combustor exit. The precise value of the stoichiometric O₂ limit at the inlet is given by the O₂ consumption of the GT (ΔO_2 GT) and can be expressed as function of the overall air fuel ratio (AFR).

Therefore, for a given CO₂ at the GT exit, the O₂ at inlet differs depending on the GT. For example: The reheat engine with two combustors and consequently a low AFR already has higher ΔO_2 GT and therefore CO₂ content at the exhaust even without FGR. The difference in O₂ consumption is indicated as ΔO_2 -RH. On the other hand to obtain a given (demanded) CO₂ exit content allows the reheat GT to run with more O₂ at the inlet compared to a single combustor engine having a lower ΔO_2 GT. This is depicted as ΔCO_{2ex} -RH in Figure 2 and leads to less challenging conditions (more O₂) at the first combustor at comparable FGR conditions.

As stated before the GT-operation with FGR is limited not by the ultimate stoichiometric limit but already by the combustor performance in terms of stability and incomplete burn out indicated by a steep increase of CO and unburned hydrocarbons. In the case of the reheat GT these two limits are separated and can be addressed in the two combustors separately: The reduced O₂ at the inlet is limiting the EV combustor (although not as much as a single combustor GT). The limit of the stable operation has formerly been stated to be around 18-16% [3, 12] although much lower O₂ inlet values seem feasible according to recent testing on EV burners [13]. A reheat GT contains a high pressure turbine between first and second combustor [10] and therefore compared to a single combustor GT runs at higher pressure and temperature. In general the higher O₂ inlet content with FGR, but also the higher pressure and temperature of the reheat GTs first combustor are beneficial factors leading to an the increased stability of the combustor.

In the sequential combustion system CO-emissions in the EV-combustor are not relevant to the GT exit emissions, which are completely determined by the SEV combustion behaviour. This shifts the problem of GT-operation to the SEV, which runs stable in auto ignition mode due to its high inlet temperature and is not affected by lean blow out problems. The O₂ level at the SEV inlet is between GT inlet and exit in Figure 2. The O₂ at combustor exit lying below the content at the GT exit can be attributed to the cooling air requirement. The focus of the present work will therefore lie in the CO emission behaviour of the SEV-combustor.

Experimental test rig

Since the effects of FGR on NO_x and CO formation are highly pressure dependent atmospheric testing and extrapolation from atmospheric results to engine pressure is of limited use especially for FGR applications. Therefore the tests under real pressure conditions are essential. The experiments were conducted using full scale engine hardware at full engine pressures at the HBK-2 test facilities at DLR in Cologne, Germany. For SEV tests a dedicated test rig (Figure 3) is mounted and operated as integral part of the Alstom development process allowing single SEV burner tests at full scale simulating the GT conditions as close as possible. To obtain SEV inlet conditions the hot gas generator is operated with an EV burner as shown in (Figure 3). The temperature and pressure drop across the high pressure turbine is simulated to some degree by flow blocking rods and adding a certain amount of dilution air to the hot gas to match the temperature and gas composition at the SEV inlet.

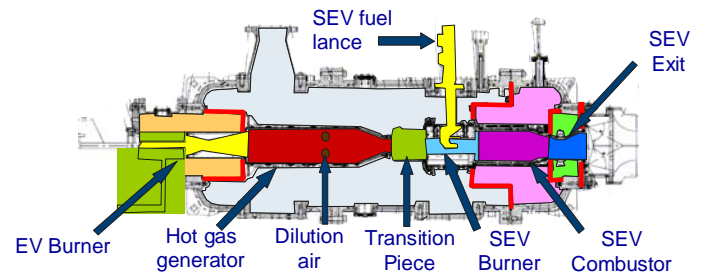


Figure 3: Schematic drawing of the hot gas path of the SEV rig compared to the GT architecture.

Since it was not economically viable to recirculate and cool down exhaust gases and for increased test rig flexibility the oxidant stream was generated synthetically. The FGR conditions were simulated by using vitiated air for the inlet condition of the EV hot gas generator. To set the gas compositions simulating FGR ratios of the GT the compressor inlet air was mixed with gases from tanks of cryogenic liquefied N₂ and CO₂. The synthetic oxidant stream then enters the hot gas generator and dilution air. The produced hot gas is mixed with dilution air to match the SEV inlet conditions as expected for the GT. With the

exception of NO_x , which would accumulate in the GT by recirculation, all combustion relevant species can be matched. To have full control over the mass flows several emission measurements had to be taken at different locations and careful balancing was required. The equipment and approach are similar to the one used for EV testing [13]. Care has to be taken with analysing the SEV generated NO_x being the difference of the absolute amount at SEV exit and inlet. As fuels methane rich natural gases have been used. To simulate C2+ containing fuels blends of with ethane /propane mixtures were used. For a reference pure methane was also used.

The flame has been visualised through a UV-fibroscope (a fibre bundle of 30000 UV transparent fibres) in a water-cooled optical probe manufactured by Alstom. The flame images were taken using a UV-sensitive ICCD camera to investigate the flame position and shapes detecting OH^* chemiluminescence occurring in the UV range. To be sensitive to the flame position, which is driven by the auto ignition process, the probe was mounted to obtain a view from the side perpendicular to the flow. To ensure that heat release indicating the flame position is detected the light from the fibre bundle was passed through an optical filter (DUG11X) limiting to the UV part of the flame emission. With this filter the detection of light caused by the flame is maximised and the sensitivity to other light sources in the combustor (black body radiation) is reduced to a minimum.

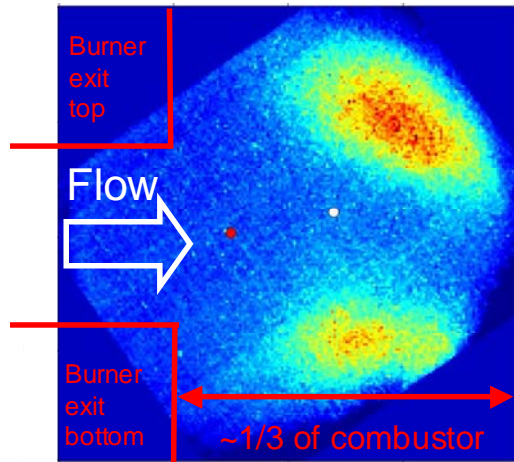


Figure 4: Flame image from averaged ICCD with combustor dimensions indicated in red.

An example image is shown in Figure 4. The flow direction is from left to right and the image only shows the first part of the combustor. The red point represents the first part of a rising intensity along the central part of the images and the white dot indicates the centre of mass of the detected intensity. Both measures can be interpreted to indicate the flame position. Note that the circular image of the fibre bundle does not illuminate the corners of the CCD chip and leaves the corners dark.

Results and discussion

The tests were conducted at conditions simulating base load over the full range of FGR ratios from no FGR to the stoichiometric limit. For each inlet composition the SEV T_{flame} and $T_{\text{SEV_in}}$ was varied to obtain a variety of benchmarking results. No unexpected instabilities were observed at normal operating conditions over the whole range. To study the effects of fuel reactivity several fuels were tested.

The NO_x emissions are plotted as emission index EMI_NO_x [g NO_2 per kg fuel] from the net SEV NO_x values and SEV fuel as discussed in [8]. This enables the evaluation of the SEV as a combustor component and allows accurate predictions of the engine behavior by using an appropriate model. The common calibration of NO_x values to 15% O_2 is valid only if the flue gases (including NO_x) are really recirculated like on the GT or a rig with actual recirculation, but not for test rigs using vitiated air (like this experiment), since the low O_2 values in the latter case are not obtained by O_2 consumption but by the simulated inlet gas composition and NO_x in that case is not carried over.

Since the CO at the GT exit are determined by the SEV only and the CO levels are not influenced by incoming CO through either FGR or EV combustor the CO can meaningfully be shown as calibrated values (i. e. 15% O_2) for the exit O_2 of the rig. These O_2 exit values are representing the GT state in terms of FGR and power and are representing the combustor performance most adequately as component for a FGR-GT plant. For NO_x the more conventional plot vs. T_{flame} is chosen. NO_x are shown as emission index SEV EI [g NO_2 / kg fuel] for the SEV combustor.

NO_x emissions

The measured SEV- NO_x -emissions are presented in Figure 5 vs. normalized adiabatic $T_{\text{flame}} / T_{\text{ref}}$ for several FGR cases (no, medium and high FGR) at the GT inlet as SEV_EI [g NO_2 /kg fuel] values normalized to the reference case (without FGR). Without FGR the NO_x emissions of the SEV increase with increasing T_{flame} . Under FGR conditions the NO_x values are lowered with decreasing O_2 . Note that at low O_2 and high T_{flame} the combustor is operated in a near stoichiometric regime, which is overall rich and does not exhibit stability problems. The NO_x emissions show very little dependence on $T_{\text{SEV_IN}}$ and fuel composition (The data are omitted here for clarity).

With increasing FGR not only the value but also the gradient of the produced NO_x (with T_{flame}) reduces resulting in a reduced impact of inhomogenities on NO_x . This indicates the potential to increase the operational flexibility by operating at locally higher firing temperatures. This observation is according to expectations and nicely confirms the experimental and theoretical findings of several groups [6, 8, 9, 13]. With a

model as described in [8] the NO_x emissions can also be described semi-quantitatively with good accuracy. Here we will present only a qualitative description of the observed results.

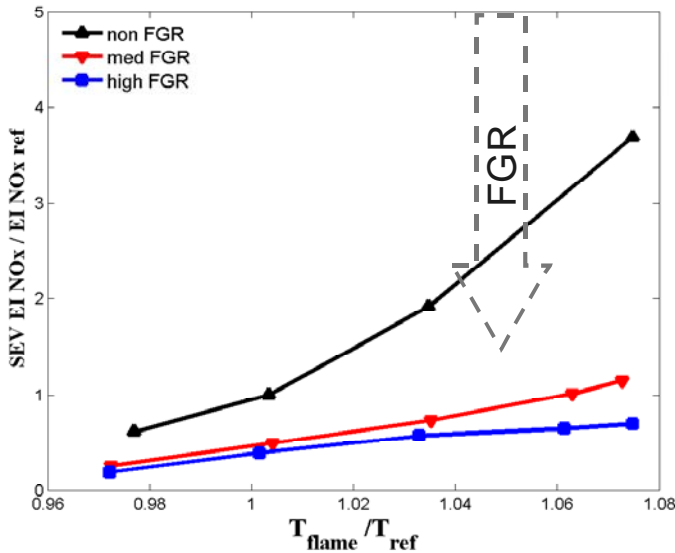


Figure 5: Measured SEV net emissions (EMI_NO_x) for different oxidizer compositions and relative T_{flame}.

As pointed out before the NO_x reduction is due to a combination of several possible effects:

- Low post flame rates according to Zeldovich's path at reduced O₂ and O-radicals levels.
- Low maximum stoichiometric T_{flame} resulting in a reduced penalty due to the unmixedness effects which typically still remain even for GT premix burners like the SEV, which is operated at high velocities and short mixing times. The penalty is less significant for FGR cases since the NO_x production depends exponentially on temperature.
- The regions of higher fuel concentration associated with the unmixedness are O₂ deficient and switch to a regime of rich combustion where the NO_x are locally even reduced due to reburn chemistry, which can be expected [8] by kinetic reasoning to be acting under SEV conditions.
- Due to the slowed down auto ignition kinetics resulting from the low O₂-contents at FGR conditions the flame is located further downstream. This results in shorter residence time for post flame NO_x production and improved time for fuel air mixing at the location of the flame.

These effects can be explained using Figure 6 where unmixedness is assumed as a generic probability density function (pdf) represented by a Gaußian distribution (blue lines), which is plotted vs. fuel mass fraction (y_f). At given load the mean fuel mass fraction (white line) remains almost constant with changing FGR, since the fluid properties and the power settings of the GT vary only

slightly with FGR [11]. The colors represent normalized adiabatic flame temperature. The residual O₂ levels in the inlet air changes with the FGR ratio resulting in changing stoichiometry over the whole range of combustion. The thick black line resembles the hottest possible temperature at near stoichiometric condition. Consequently also the range of possible temperatures sampled by the residual unmixedness at the position of the flame (assumed constant here) reduces with FGR. With the pdf resembling mixing quality at the flame position by a single burner characteristic parameter emissions can be well predicted for NO_x emissions and CO in certain condition as will be explained later.

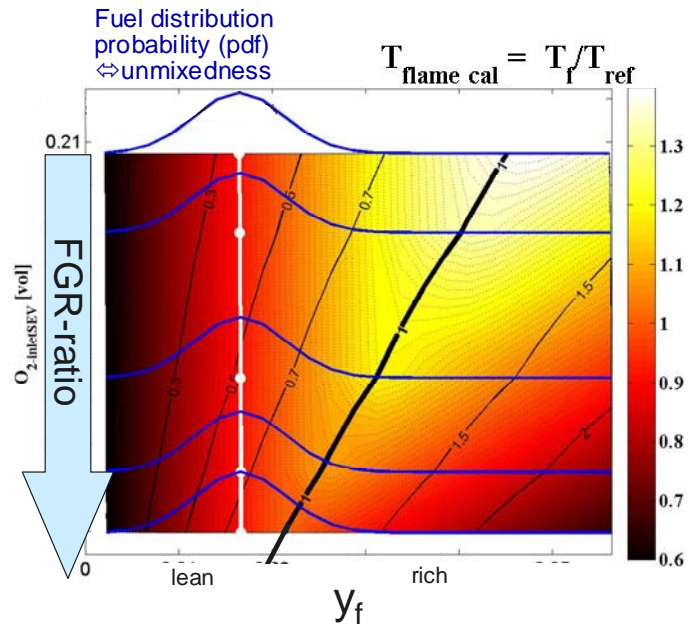


Figure 6: Map of non-dimensionalized flame temperature $T_{f,cal} = T_{flame} / T_{ref}$ as a function of fuel mass fraction y_f and O₂ concentration (% vol at GT inlet).

Consequently the effect of mixing in the flame front on NO_x emissions becomes less relevant for the combustor design with increasing FGR. It has been shown [8] that for perfect premixing the already low NO_x emissions even increases with FGR due to increased size of reaction zones and changes in the relevance of the kinetic NO_x formation pathways. The observed NO_x benefit due to FGR is continuing to exploit the physical and chemical advantages that a sequential combustor within a reheat combustion system already offers with respect to a single combustor [10].

CO emissions

The measured results for the CO emissions are presented in Figure 7 normalised to their equilibrium values at the corresponding exit conditions plotted vs. the O₂-concentration at the SEV exit (normalised to the reference non FGR case). The CO emissions are

reasonably low (near the equilibrium value) over a wide range of operating conditions (FGR and T_{SEV_IN} , T_{flame}). At extreme conditions and unfavourable combinations of these parameters (high FGR, low T_{SEV_IN} and low T_{flame}) however the CO emissions can rise quickly by several orders of magnitude. In that plot the CO values for different T_{flame} and O_2 exit collapse on one graph around 1 for high values of O_2 exit and high T_{SEV_IN} . At low T_{SEV_IN} the CO-rise starts at higher O_2 exit concentration – most clearly visible for the lowest T_{flame} .

To interpret the results some general remarks discussing CO emissions shall be revisited:

In GTs CO emissions are usually occurring at low loads when p_{inlet} , T_{inlet} and $T_{hot\ gas}$ are lower than at high loads slowing down the CO burn out kinetics. Generally the condition for CO burnout in the SEV can be formulated in equation (1).

$$t_{res} > t_{ign}(T_{SEV_IN}) + t_{CO_burnout}(T_{hotgas}) \quad (1)$$

While the flame position of the SEV auto ignition flame depends on the inlet conditions the burnout time for complete CO oxidation depends on the conditions at the end of the combustion process determined by $T_{hot\ gas}$ and the exhaust composition. If equation (1) is not fulfilled increased CO emissions are expected due insufficient CO-burnout and the CO emission is referred to as “kinetically controlled”.

The final state of oxidation in a combustor is not complete conversion to CO_2 , but is given by the equilibrium state, which for low loads and T_{hotgas} corresponds to a very low CO value. The equilibrium value of CO is determined by the combustion pressure and the conditions at the combustor exit (T_{hotgas} , CO_2 , O_2 and stoichiometry ϕ). Several trends are relevant for the understanding of CO formation:

- At increased T_{hotgas} the CO-equilibrium concentration increases. (thermodynamic control).
- With increasing FGR the CO-equilibrium concentration increases due to the increased CO_2 and decreased O_2 . (CO_2 enrichment-effect).
- The stoichiometric maximum T_{flame} decreases with increasing FGR as already seen in Figure 6. This results in a higher probability for over-stoichiometric compositions. Even when the equilibrium is reached for these parts of the flame the CO values increase drastically since these equilibrium values in the rich are several orders of magnitude higher than for fuel lean conditions (stoichiometric effect).
- Only at low temperatures and pressures is the residence time insufficient for CO oxidation and kinetic CO emissions arise. (kinetic control).

To analyse the different causes for the measured emissions the presentation in Figure 7 is useful since it

becomes obvious (for high O_2 exit content (on the right)) that the reactor residence time at high T_{SEV_IN} is sufficient for CO oxidation (reaching the equilibrium value = 1) while for low T_{SEV_IN} (lower graph) the kinetic contribution determines the CO production. The region of kinetic control according to equation (1) is indicated by the red arrow. At low T_{SEV_in} the kinetic contribution (deviation from the equilibrium) to CO emission is dominating for the lowest T_{flame} while the values for the highest T_{flame} are resembling the graphs of the upper plot showing the more reactive cases at higher T_{SEV_in} .

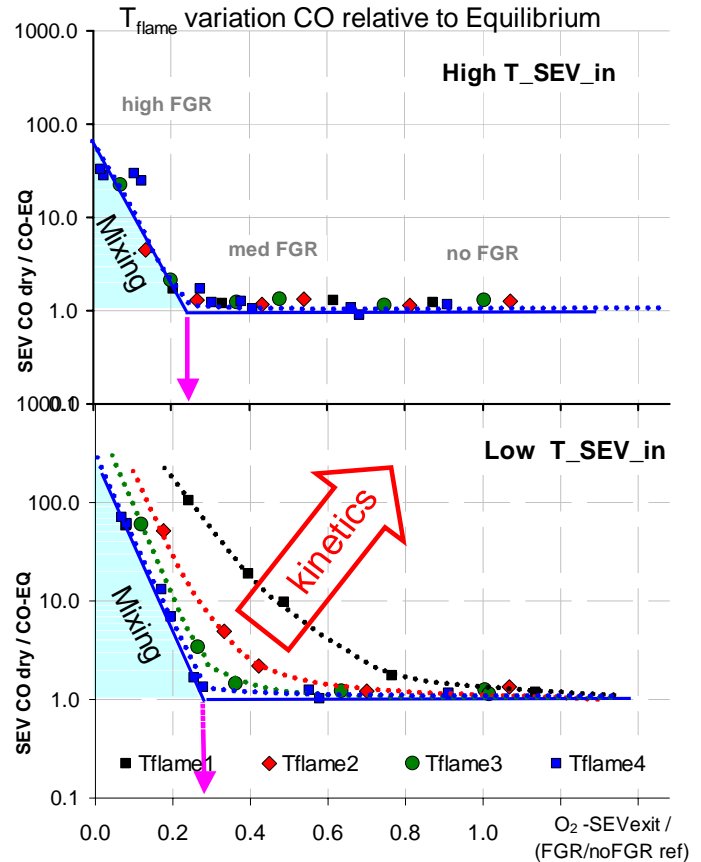


Figure 7: Measured CO emission values plotted normalised to the equilibrium values vs. non-dimensionalised O_2 exit concentration. Indicated is the area of mixing limited CO, a minimum O_2 exit level for SEV mixing and the onset of kinetic CO production.

The second deviation from the equilibrium line at occurs only at very low O_2 exit concentrations. The onset of the CO is similar for all cases and seems to be determined by the same parameters. The magenta colored arrow indicates an arbitrarily drawn point of reasonably low exit O_2 concentration where the emissions clearly start deviating from the equilibrium curve. Since the conditions of the combustor allow sufficient time for oxidation (ruling out the kinetic effect at least for the “high T_{SEV_in} ”) the reason for the increase must be the local

lack of oxygen in combination with mixing effects on the test rig. These regions are indicated by the light blue shaded triangular regions indicating the increasing CO according to the mixing effect. The results can be fully explained by the mixing quality before the end of the combustor even when full equilibrium composition for each flame region as is indicated in the following. The fact that all “CO vs. O₂-exit” plots (also for varied T_SEV_in and fuel reactivity- not shown here) exhibit the same boundary (shaded light blue region) toward low O₂-concentration strengthen this interpretation.

With this explanation it also becomes evident that for further increased reactivity the CO emissions do not further increase since they are not kinetically controlled but rather determined by the mixing at the end of the combustor, which comprises of Inhomogenities from the individual burner as well as the annular combustor.

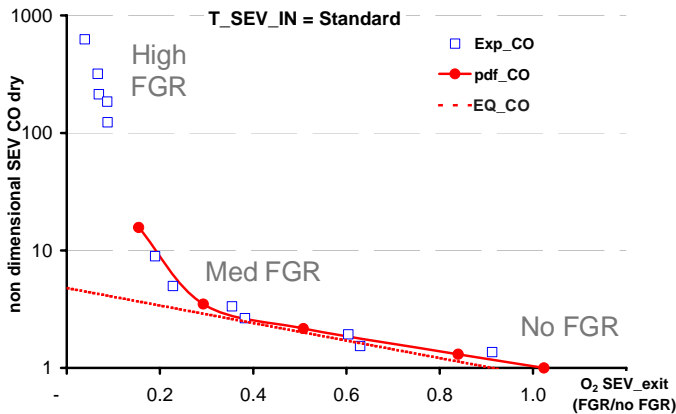


Figure 8: Normalised experimental data compared to a pdf model considering equilibrium CO values at high FGR.

Already very small contributions from the over stoichiometric regions due to residual inhomogenities can contribute significantly to the CO emission of a combustor. This is shown in Figure 8 and can be modeled in an approach similar the one used for NO_x emission values described in [8] by a pdf approach using unmixedness near the flame front. For CO emissions the relevant location is the combustor exit where the mixing is much better although not perfect and CO values are given by the equilibrium values for different stoichiometries. Plotted are normalized CO emissions vs. O₂ exit concentration normalized to the exit concentration at non FGR operation.

With the very steep increase in CO equilibrium values at the stoichiometric point (where O₂-exit concentration approaches zero) already small percentages of rich combustion gases can explain the observed increase of CO. The residual unmixedness of combustion gases is in agreement with results from the mixing quality obtained from CFD simulation: the influence of the flue gas recirculation operation on the mean aerodynamics and

mixing characteristics of the SEV combustor was assessed using CFD simulations. The simulations were performed using an advanced combustion modeling approach developed for auto-ignition flames, and well adapted to the conditions of the SEV combustor [14]. More details about the CFD modeling can be found elsewhere [15].

Given the high levels of mixing achieved in the burner, the flame thickness is rather large. Consequently, the heat release is well distributed, and the impact of the flame expansion on the mixing characteristics is small. In particular, the unmixedness at the exit of the combustor is solely a function of the burner and its mixing quality.

CFD modeling results are shown in Figure 9: The SEV burner on the left and an iso-surface of a low O₂ concentration at the combustor end (on the right) where the flame is burned out and mixes hot products with leaner parts of the flame are presented. The region within the indicated iso-surface are lowest in O₂ and are most likely to be responsible for high CO emissions due to the stoichiometric effect. The emissions are sampled at a position resembling the turbine at the right end of the figure. If the zone inside the indicated area is considered to be critical for CO burnout due to lack of O₂ the observed data for high FGR can be explained for high loads from equilibrium and mixing studies alone.

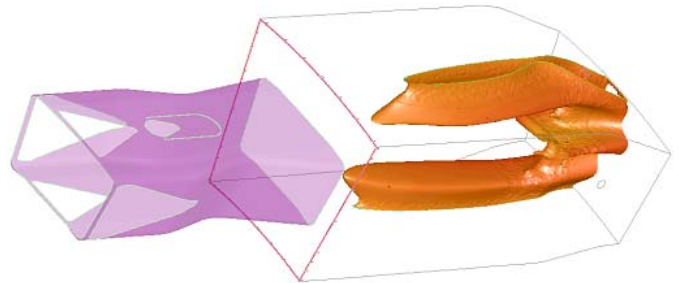


Figure 9: CFD simulation of SEV combustor: plot of O₂ iso-surface for 0.5% for high FGR near base load.

Unlike at part load conditions, where the lower temperatures lead to kinetic control of the CO emissions, kinetics are not limiting the CO oxidation in this case. Although the obtainable FGR ratios with the reheat system incorporating EV and SEV combustors reach high recirculation ratios (expressed as CO₂ at the GT exit) possible improvements extending the FGR range would require improving the mixing performance of the sequential combustor.

At high FGR the operation can be limited by high CO emission for similar reason that for non-FGR cases NO_x are setting limits for very high T_{flame}. For low loads and reduced temperatures kinetic effects are limiting the CO burn out. At this conditions operating at higher inlet temperatures can extend the operation regime without negative impact on power output as explained elsewhere [16].

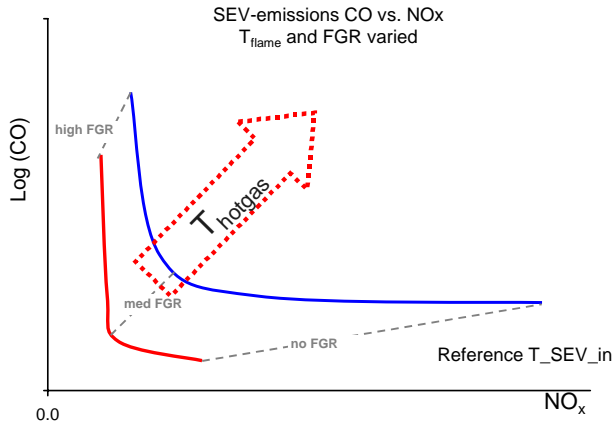


Figure 10: Schematic SEV emissions: CO and NO_x combined: Coloured lines indicated groups of common T_{flame}.

For the engine operation a compromise between CO and NO_x emissions needs to be found. This is shown in Figure 10, where CO emissions are plotted logarithmically vs. SEV NO_x. With increasing T_{flame} both emissions increase. The increase of FGR shifts high NO_x to high CO emissions passing a point where both emissions are within acceptable limits. The presented data encourage the operation of GT with FGR at the current GT conditions with low NO_x emissions yielding some increase in operational flexibility with respect to increased local firing temperatures. It is clear from Figure 10 that for FGR operation conditions can be found, where emissions of both, CO and NO_x, are reasonably low.

Reactivity at FGR conditions

To study the reactivity changes that are caused by the reduced O₂ levels at FGR, flame images were recorded and are shown in Figure 11. With fuel being injected into the hot air on the left side of the observable region the flame moves upstream according to its expected reactivity. The images resemble conditions varied for the main parameters for SEV combustion: O₂ content at inlet (FGR) and fuel composition expressed as C2+ content in methane rich natural gas. C2+ is sum of higher alkanes (C_nH_{2n+2}) in the gaseous fuel. The C2+ content was obtained by mixing an ethane / propane mixture with natural gas to obtain the desired C2+ value

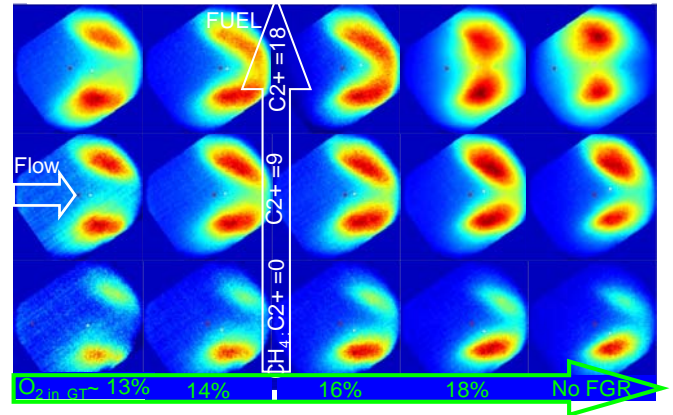


Figure 11: Flame images for varied inlet composition resembling decreasing FGR from left to right and increased reactivity due to increased C2+ value of the fuel. T_{flame} and T_{SEV_IN} are kept constant.

The images in Figure 11 are scaled for intensity from minimum to maximum to enable a localization of the heat release zone for all cases. The view field of the camera - fibroscope is limited to about 1/3 of the combustor clipping part of the post flame region. The over all intensity of the flame as detected in the ICCD increases strongly with T_{flame} and decreases less strong but clearly detectable with FGR ratio. The intensity increase is also clearly visible when flames of similar position are compared avoiding the artificial dependence of flame movement on the intensity result if the flame moves out of the observation window.

All images in Figure 11 correspond to stable operating points and although the flame position is clearly varying with FGR and fuel composition no blow out was occurring. It is actually a remarkable property of this flame that the stability is not very dependant of the exact flame position. Flames of lower reactivity move downstream in the combustor and are more likely to yield higher CO especially with FGR. In the lower row in Figure 11 the least reactive fuel (pure CH₄) is used and the flame is already located downstream of the burner. Changes in flame position are hard to detect with the given view field. The flame is only slightly moving downstream when O₂ at the inlet is reduced indicating that a flame stabilization other than a pure auto ignition mechanisms is also actively keeping the flame lit. This is also supported by the observation that the low reactivity flames appear to move not only downstream, but also towards the outer regions away from the center line.

For the higher C2+ values the flame is clearly following the trend of higher reactivity with C2+ and with O₂ content by moving upstream towards the combustor according to a reduction in τ_{ignition}. The calculated values are shown in Figure 12 as function of fuel composition and inlet air composition.

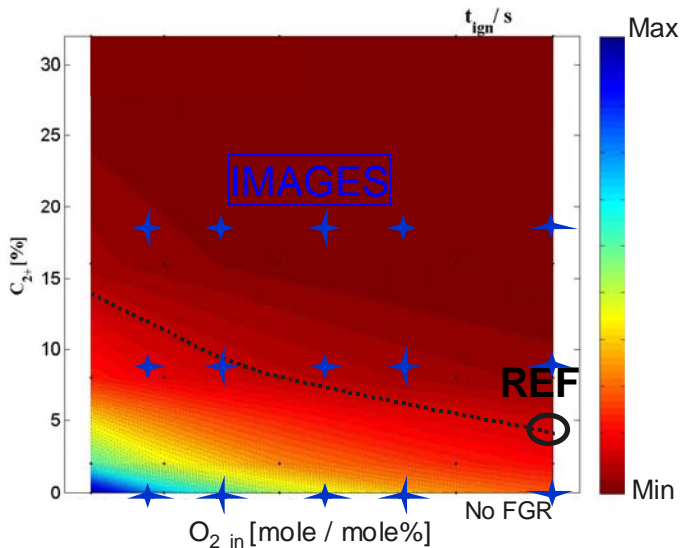


Figure 12: Simulated ignition times (GRI 3.0) vs. C₂₊ content and O₂ content at the GT inlet.

The change of flame position or shape with T_{flame} and T_{SEV_IN} is small although the CO emissions can vary significantly indicating that SEV reactivity can be observed with flame images only to some degree from this view angle.

Conclusion

The feasibility to operate a GT under FGR conditions up to high FGR ratios is demonstrated. The prospect for reheat engines is particularly promising considering the increased flexibility of the sequential combustion system. One of the advantages is the split of the two limiting factors for FGR operation (stability and CO emissions) in two separate combustion systems - namely the EV and the SEV combustors. The sufficient EV stability under FGR has been demonstrated earlier [13] especially the conditions of the reheat architecture (high P_{K2} and T_{K2} and O₂ inlet) support EV operation at high FGR ratios.

The FGR feasibility for a GT with CCS should be benchmarked in terms of exit CO₂ rather than FGR ratio alone since the latter is highly dependent on the overall AFR of the GT and therefore, on the GT architecture. In that respect sequential combustion systems or engines with ultra high firing temperatures are already utilizing the combustion air more efficiently producing higher CO₂ content at the GT-exit. With a sequential combustion system (like the Alstom reheat engines GT26/GT24) the benefits that FGR offers are already utilized to some extent. Extending this further by actually recirculating the flue gases can be done without major modifications to the GT.

This work focuses on the emissions of the sequential combustor (SEV) demonstrating operation at high FGR ratios if benchmarked against CO₂ content at the GT-exit. Especially utilizing the flexibility in operation of the reheat

engines offers great opportunities for a wide operating range on the GT.

In terms of CO emissions a mechanism uncommon for GTs is identified explaining the increased CO emissions at very high FGR ratios even at high T_{hotgas} related to the mixing quality at the combustor exit. With the basic understanding and the fundamental operation limits at FGR obtained at engine pressures the engine operation is found also possible at lower loads.

The decrease in NO_x produced in the EV and SEV with FGR follows expectations and preceding results. This experimental verification on full-scale burners and pressures and the results concerning stability and emissions as well as the thermal analysis [11] allow promising prospects for the use of this technology in GT applications.

REFERENCES

- 1 IPCC, 2007: Summary for Policymakers. In: Climate Change 2007: The Physical Science Basis. Contribution of Working Group I to the Fourth Assessment Report of the Intergovernmental Panel on Climate Change [Solomon, S., D. Qin, M. Manning, Z. Chen, M. Marquis, K.B. Averyt, M. Tignor and H.L. Miller (eds.)]. Cambridge University Press, Cambridge, United Kingdom and New York, NY, USA.
- 2 IPCC, 2005: IPCC Special Report on Carbon Dioxide Capture and Storage. Prepared by Working Group III of the Intergovernmental Panel on Climate Change [Metz, B., O. Davidson, H. C. de Coninck, M. Loos, and L. A. Meyer (eds.)]. Cambridge University Press, Cambridge, United Kingdom and New York, NY, USA, 442 pp
- 3 Bolland O., Mathieu P., "Comparison of Two CO₂ Removal Options in Combined Cycle Power Plants", Journal of Energy Conversion and Management, Vol. 39, No. 16-18, pp. 1653-1663 (1998).
- 4 Roekke P. E. and Hustad J. E., "Exhaust gas recirculation in gas turbines for reduction of CO₂ emissions; combustion testing with focus on stability and emissions", International Journal of Thermodynamics, vol. 8, pp. 167-173 (2005).
- 5 Griffin T., Buecker D., Pfeffer A., "Technology Options for Gas Turbine Power Generation With Reduced CO₂ Emission", ASME Journal of Engineering for Gas Turbines and Power, 130, 041801 (2008).
- 6 Ito E., Okada I., Tsukagoshi K., Miyama A., Masada J. "Development of Key Technologies for the Next Generation 1700C-class Gas Turbine", ASME paper GT2007-28211, Montreal, Canada (2007) and GT2009-59783, Orlando, Florida (2009). GT2010-23396, Glasgow, Scotland (2010).
- 7 Evulet A. T., Elkady A. M., Branda A. R., Chinnb D., "On the Performance and Operability of GE's Dry Low NO_x Combustors utilizing Exhaust Gas Recirculation for

Post-Combustion Carbon Capture”, Energy Procedia 1 (2009) 3809–3816.

8 Guethe F., de la Cruz García M., Burdet A., „Flue Gas Recirculation in Gas Turbine: Investigation of combustion reactivity and NOx emissions”, ASME paper GT2009-59182, Orlando, Florida (2009).

9 Li H., ElKady A. M., Evulet A. T., “Effect of Exhaust Gas Recirculation on NOx Formation in Premixed Combustion System”, GE –AIAA 2009-226 .

10 Guethe F., Hellat J., Flohr P., “The reheat concept: the proven pathway to ultra-low emissions and high efficiency and flexibility”, ASME paper GT2007-27846, Montreal, Canada, (2007) and J. Eng. Gas Turbines Power 131, 021503 (2009).

11 Sander F., Carroni R., Rofka S., Benz E., Nicklas M., “Flue Gas Recirculation In A Gas Turbine: Impact On Performance And Operational Behavior”, ASME paper GT2011-45608, Vancouver, BC, Canada (2011).

12 ElKady A., Evulet A., Brand A., Ursin T. P., Lyngghjem A., ASME paper GT2008-51152, Berlin, Germany (2008).

13 Lachaux T., de la Cruz Garcia M., Winkler D., Burdet A., “Combustion under Flue Gas Recirculation Conditions in a Gas Turbine lean premix Burner”, ASME paper GT2010-23233, Glasgow, Scotland (2010).

14 Ivancic B., Brandt M., Flohr P., Polifke W. & Paikert B., “Auto.Ignition and Heat Release in a Gas Turbine Burner at Elevated Temperature”, ASME Turbo Expo 2004, GT2004-53339.

15 Düsing, K. M., Ciani, A. and Eroglu, A., "Effect of Mixing Quality on NOx Emissions in Reheat Combustion of GT24 & GT26 Engines", ASME Turbo Expo, GT2011-45676.

16 Ciani A., Eroglu A., Güthe F., Paikert B., "Full-Scale Atmospheric Tests of Sequential Combustion", ASME Turbo Expo, GT2010-22891.